Jour. Fac. Sci., Hokkaido Univ., Ser. IV,
vol. 19, nos. 1-2, March, 1979, pp. 241-255.

THE BASIC PLUTONIC ROCKS OF THE HIDAKA METAMORPHIC BELT, HOKKAIDO. PART II

The Ameyama Layered Gabbros in the Tokachi Province.

by

Seiji Hashimoto, Sumio Miyashita and Jin-ichiro Maeda

(with 14 text-figures and 3 tables)

(Contribution from Department of Geology and Mineralogy,
Faculty of Science, Hokkaido University, No. 1639)

Abstract

The occurrence of cumulus gabbro in the Hidaka Metamorphic Belt has been noted in the Western Zone of the Metamorphic belt as cumulus series of dunite-wehrlite-troctolite-olivine gabbro-anorthosite and various amphibolites which were obducted westward (Miyashita and Hashimoto, 1975). Besides the Western Zone gabbro series, many small bodies of cumulus gabbros have been known as fault bounded blocks throughout the whole metamorphic belt in the Axial and Eastern zones (Hashimoto, 1975).

The Ameyama gabbro which occurs as an outlier of the metamorphic belt, is described and is compared with the Western Zone gabbros.

Diabase which is accompanied by the Ameyama gabbro is also described. The chemical characteristic of the diabase show that it is nearly the same as the Hidaka Western Marginal Zone diabases but a slight difference in the trend of differentiation is revealed.

Introduction

Ameyama is a small hill in the Tokachi Plain, some 20 km to the east of the Northern Hidaka Range. The hill is composed of coarse-grained gabbros in which cumulative texture is present. The body of fine-grained diabase is accompanied by the gabbro but the poor exposure due to the covering of the Pliocene and Pleistocene deposits hindered to make clear the relation between the both rocks. However, the occurrence of the crushed gabbro and slaty sediments in the southside of the hill suggests that the gabbro and diabase seem to occur as fault bounded blocks which were pushed up into the Lower Hidaka Supergroup sediments considered to be Triassic or older in age (Fig. 1).

Petrography

The Ameyama gabbros show faint cumulative layering dipping gently to the north-northeast. The Ameyama rocks can be classified into three groups of gabbro by modal analyses. They are wehrlitic gabbro, troctolite and gabbros with or without olivine (Fig. 2). The lowest part consists of wehrlitic gabbro and olivine rich troctolite which is gradational to troctolite and gabbros upward, although recurrent of the darker layers may occur. As far as the exposures are observed, troctolite and gabbros are the chief constituent rock types. Dominant layering does not exist in these rocks.

Wehrlitic gabbro: Wehrlitic gabbro occurs as indistinct layers several meters to decimeters in thickness. The cumulus mineral is rounded or idiomorphic olivine, 3 to 5 mm in diameter. No zoning is present. The occurrence of the kink band indicates strain effect

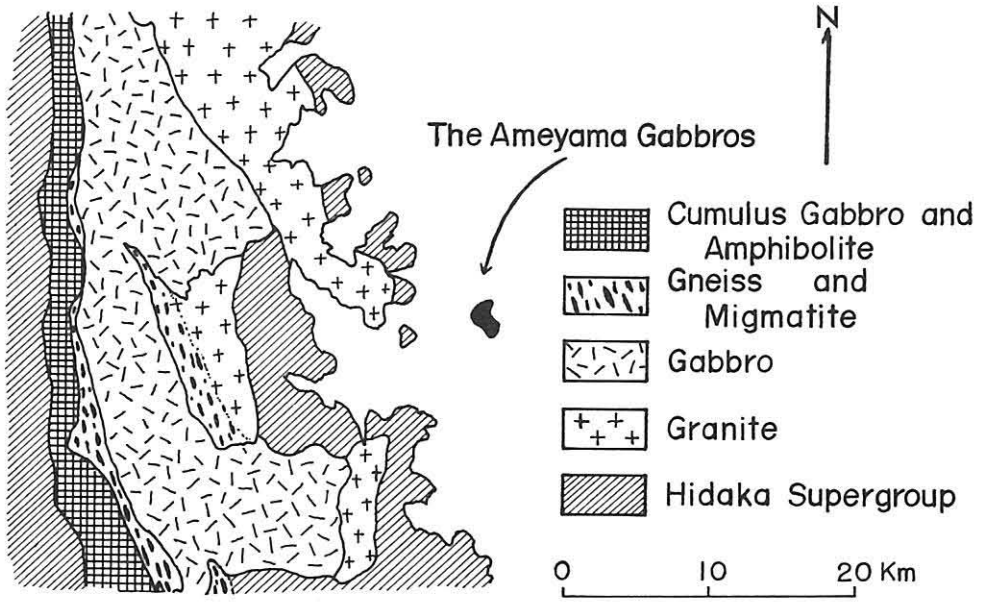

Fig. 1 Simplified geologic map showing the location of the Ameyama gabbros.

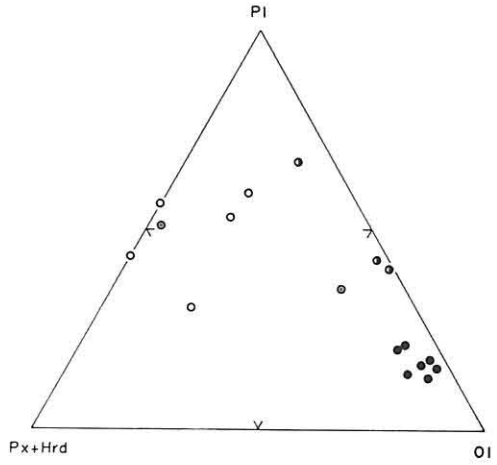

Fig. 2 Modal Ol-Pl-Px+Hrd plots of the Ameyama gabbros.
Filled circle: Wehrlitic gabbro. Half filled circle: Troctolite. Circle with dot: Pegmatoid. Open circle: Olivine gabbro and gabbro. The same symbols are used in all diagrams.

due to the uplift. It is considerably serpentinized along the margin and cracks to be transformed to chrysotile and magnetite. Amount of cumulus olivine is about 81 to 76 percent. Intercumulus mineral is plagioclase, 16 to 12 percent, and clinopyroxene, 10 to 3 percent. Small amount of orthopyroxene and brown hornblende also exist. Plagioclase shows zoning, most of which has been saussuritized. Clinopyroxene showing thin exsolution lamellae, exhibits poikilitic habit. Zoning is common but not distinct. Orthopyroxene is chloritized from the margin. Brown hornblende has distinct exsolution lamellae of rhombic amphibole. Minor amount of biotite is present being associated with small grain of chromian

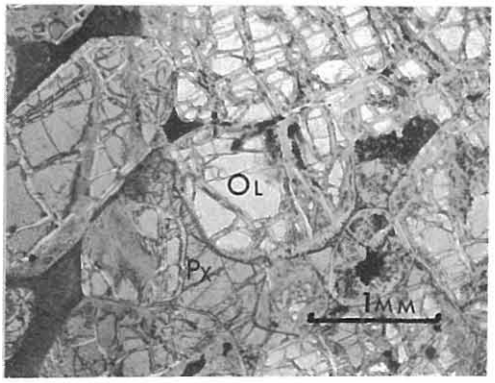

Fig. 3 Wehrlitic gabbro. Texture is ortho- to meso-cumulate.
Ol: Olivine. Px: Clinopyroxene. Plagioclase is saussuritized. The scale is same in all photomicrographs.

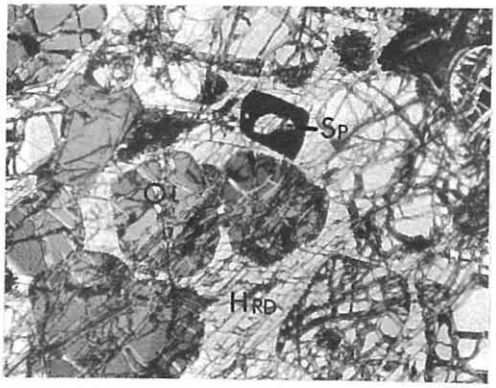

Fig. 4 Brown hornblende in wehrlitic gabbro.
Hrd: Hornblende. Sp: Chromian spinel.

spinel which is enclosed by olivine and pyroxene (Fig. 4).

The mineral assemblage and the texture suggest that during consolidation there was no considerable exchange of the components between the trapped liquid and the magma, therefore wehrlitic gabbro should be ortho to mesocumulate (Wager et al., 1963).

Troctolite: The layer of wehrlitic gabbro grades into troctolite on either side. Troctolite near wehrlitic gabbro is rich in olivine which is also gradational to normal troctolite having moderate amount of olivine, 60 percent, and to plagioclase rich troctolite, olivine 25 percent. Olivine, 5 to 3 mm in diameter, is the mineral cumulated. It is granular to subidiomorphic. No zoning is observed. Plagioclase, about 40 to 65 percent, is subhedral to anhedral and is weakly zoned. It sometimes encloses small olivine. Idiomorphism of plagioclase is more pronounced in plagioclase rich troctolite. Therefore it should be cumulus as well as intercumulus. Clinopyroxene appears as intercumulus forming poikilitic crystal up to 10 mm in diameter, and shows very thin lamellae. Zoning is more or less present. Some clinopyroxenes are partly replaced by brown hornblende coaxially. Clinopyroxene occurs, sometimes, as very thin rim between olivine and plagioclase.

Olivine gabbro: Olivine gabbro comprises two subtypes; subtype 1 olivine gabbro is characterized by the cumulus plagioclase as well as by olivine and also the most of pyroxene. Subtype 2 has the cumulus plagioclase only. The constituent mineral is the same in both subtype rocks.

Subtype 1 olivine gabbro, containing about 50 to 65 percent of subhedral plagioclase ranging from 5 to 2 mm in length, which often shows igneous lamination. Zoning is common. Cumulus olivine, about 20 to 25 percent, is granular or anhedral to plagioclase. Clinopyroxene mostly forms granular subhedral crystal 2 to 4 mm in diameter and is zoned. Exsolution lamellae are common. Poikilitic clinopyroxene is scarce. Cumulus plagioclase of subtype 2 olivine gabbro is subhedral to masaic granular, 3 to 2 mm in length, and is reversely zoned at the margin. Olivine occurs at the interstitial site between plagioclase,

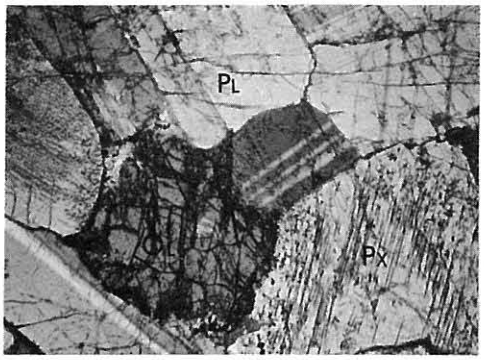

Fig. 5 Olivine gabbro. Olivine, clinopyroxene and plagioclase are cumulus phases.

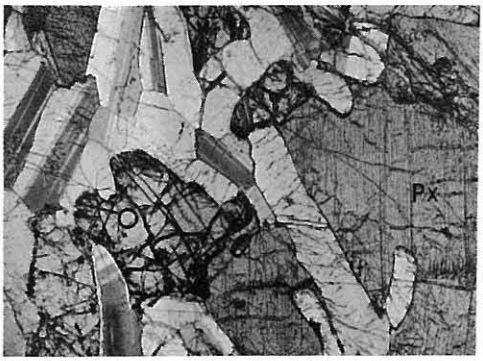

Fig. 6 Olivine gabbro. Plagioclase is a cumulus phase. Anhedral olivine and poikilitic clinopyroxene are shown.

although some granular crystals exist in plagioclase. Clinopyroxene is poikilitic, up to 10 mm in diameter, which is often rimmed by brown to greenish hornblende.

Pyroxene gabbro was found as boulders in several places in Ameyama hill. The rocks are mostly coarse-grained with subhedral plagioclase, 8 to 2 mm in length, and subophitic to poikilitic clinopyroxene replaced partly by brown hornblende which is further transformed to greenish hornblende. The igneous lamination is present. Fine-grained pyroxene gabbro consisting of xenomorphic granular plagioclase and clinopyroxene, is also present. This gabbro has coarse grained parts whose clinopyroxenes have been irregularly replaced by brown hornblendes.

The coarse-grained olivine gabbroic of gabbroic schlierens were found in wehrlitic gabbro. Although the occurrence of these pegmatoids is suggested to be formed by the segregation process, the cumulus texture is evident. Cumulus olivine, 5 to 3 mm rarely 10 mm in diameter, is enclosed by subhedral to anhedral plagioclase and subophitic clinopyroxene. Orthopyroxene and brown hornblende are present as an accessory. Faint zoning exists in clinopyroxene.

Diabase: Diabase crops out in the northern part of the hill. Most of diabase is subporphyritic having lathes of plagioclase which are 2 x 0.5 mm in size. They are zoned to have a composition An_{56} in the core and An_{30} at the margin. The groundmass shows ophitic texture composed of small, 0.3 to 0.1 mm, plagioclase lathes and ophitic clinopyroxenes which have been replaced by greenish hornblendes, Ore is abundant in many rocks. The groundmass plagioclase is zoned whose composition varies from An_{63} to An_{42}, mostly An_{56} in the core, and An_{46} to An_{30} at the rim.

Very small xenolithic inclusions are present, being shown by the aggregates made up of hypersthene and biotite which are surrounded by rims consisting of hornblende and biotite.

Mineralogy

Plagioclase: Plagioclase of the Ameyama gabbro occurs as intercumulus mineral in wehrlitic gabbro and occurs as cumulus mineral in troctolite and gabbro with or without

olivine.

In wehrlitic gabbro, the composition of plagioclase varies from An_{74} to An_{62} from the core to the margin. Plagioclase of troctolite is homogeneous and has a compositional range from An_{85} to An_{70}, of which An_{70} is most common. Plagioclase of olivine gabbro occurs as intercumulus and cumulus as well.

The cumulus plagioclase is indistinctly zoned to have composition An_{73} in the core, An_{62} in the mantle and An_{66} at the margin. The reversed zoning between the mantle and the margin is characteristic in olivine gabbro.

The intercumulus plagioclase is anhedral to cumulus olivine but has a tendency to show idiomorphism to clinopyroxene which rarely has inclusion of plagioclase. The zoning is distinct in some crystals but some others are homogeneous which have the composition of An_{61} that comprises the composition of the mantle parts of the zoned crystals. The core of the zoned plagioclase is An_{68} to An_{65} which is surrounded by the mantle whose composition is An_{61} to An_{60}. The rim is commonly present which has slighly more calcic (An_{66} to An_{63}) than the mantle.

Plagioclase of pyroxene gabbro has the composition of An_{58} to An_{62} which occasionally has a calcic core (An_{64}) and or a sodic one (An_{57}). The composition of plagioclase in the pegmatoid varies with the host rock mineral assemblage. The one which is associated with olivine rich pegmatoid, varies from An_{70} (core) to An_{65} (margin). Besides, many plagioclases are unzoned and are An_{67} in composition. On the other hand, the pegmatoid poor in olivine, has various plagioclase whose composition varies from An_{66} to An_{60} or mostly from An_{62} to An_{55}.

Olivine: Olivine of the Ameyama gabbros occurs as unzoned cumulus crystals, granular to subhedral in shape. The composition of olivine which was determined by X-ray diffraction method (Sinno and Hayashi, 1976) and EPMA analysis, shows that Fo content is high in wehrlitic gabbro and troctolite and is lower in olivine-plagioclase cumulate gabbro and is lowest in plagioclase-olivine cumulate gabbro whose olivine is subhedral to anhedral. The compositional variation is scarce in each rock. While olivine of the pegmatoid schlieren shows much wider compositional range: Wehrlitic gabbro Fo_{88}, Troctolite $Fo_{89\text{-}88}$, Plagioclase rich troctolite $Fo_{87\text{-}86}$, Plagioclase-olivine cumulate (Olivine gabbro) $Fo_{77.5\text{-}77.2}$, Olivine rich pegmatoid $Fo_{89.4\text{-}78.2}$, Olivine poor pegmatoid $Fo_{77.2\text{-}77.0}$. The chemical compositions of representative olivine are shown in Tab. 1.

Pyroxene: Pyroxene of the Ameyama gabbro is mostly clinopyroxene occuring as an intercumulus mineral. Orthopyroxene is present but very small in amount. Many clinopyroxenes and orthopyroxene were analysed by EPMA using JEOL 5A-model. The chemical compositions were tabulated (Tab. 1) and were plotted in a Di-Hd-Fs-En quadrilateral (Fig. 7). The coexisting compositions of cumulus olivine are also indicated.

Plots of intercumulus clinopyroxene of troctolite are high in Ca and Mg and are concentrated near the diopside corner. There is a notable compositional gap between those and the cumulus and intercumulus clinopyroxenes of olivine gabbro and pegmatoid which are rich in Fe and poor in Ca. In terms of Mg/Mg + Fe ratio, plots of Al, Cr and Ti content of clinopyrocenes were indicated in Fig. 8 and 9. In the troctolite intercumulus pyroxene, Al increases from the core to the margin of the crystals. The same tendency is shown in the

Table 1 Chemical composition of olivine and clinopyroxene from the Ameyama Gabbro.
T: Troctolite. P: Pegmatoid. G: Olivine gabbro and Gabbro

	Olivine				Pyroxene										
	1	2*	3	4	1	2	3	4*	5	6	7	8	9	10*	11
	Ame 13	Pip 14	Ame 3	Pip-Ame-11′	Ame 13	Ame 13	Ame 13	Pip 14	Ame 3	Ame 3	Ame 4	A-7	Pip-Ame-11′	A-1	Ame 3
SiO_2	40.4	39.7	39.7	38.6	51.9	50.6	50.9	50.5	51.3	51.5	50.5	50.6	51.3	51.1	55.0
TiO_2	0.06	0.03	–	0.01	0.60	1.16	1.11	1.43	0.76	0.80	0.81	0.65	1.00	0.62	0.01
Al_2O_3	0.04	0.22	0.01	0.05	2.67	3.38	3.45	2.81	2.89	3.17	2.94	3.65	2.79	2.69	0.42
Cr_2O_3	0.03	0.08	0.02	–	1.01	1.48	1.47	0.69	0.67	0.92	0.41	0.42	0.34	0.23	–
FeO**	11.8	13.4	19.8	20.6	3.31	3.21	3.49	3.85	5.81	6.16	6.59	6.65	6.82	5.40	15.8
MnO	0.09	0.20	0.19	0.29	0.01	0.05	0.10	0.13	0.15	0.10	0.08	0.22	0.15	0.15	0.46
MgO	47.4	45.9	40.9	39.9	16.7	15.7	16.0	16.3	16.3	16.7	15.8	16.7	16.1	15.9	28.2
CaO	0.06	0.08	0.04	0.03	23.3	24.2	23.2	24.4	21.8	20.7	22.6	20.8	21.0	23.7	0.14
Na_2O	–	–	–	–	0.34	0.52	0.43	0.39	0.35	0.41	0.31	0.31	0.30	0.39	–
K_2O	–	–	–	–	–	–	0.01	–	–	–	0.02	–	–	0.01	0.02
Total	99.9	99.6	100.6	99.5	99.8	100.3	100.2	100.5	100.0	100.5	100.1	100.0	99.8	100.2	100.1
Number of cation per 4 oxygens					Number of cation per 6 oxygens										
Si	1.00	0.993	1.01	1.00	1.91	1.87	1.88	1.87	1.90	1.90	1.88	1.88	1.91	1.89	1.98
Al	0.001	0.006	–	0.002	0.116	0.147	0.150	0.123	0.126	0.138	0.129	0.159	0.122	0.117	0.018
Ti	0.001	0.001	–	–	0.017	0.032	0.031	0.040	0.021	0.022	0.023	0.018	0.028	0.017	–
Cr	0.001	0.002	–	–	0.030	0.044	0.043	0.020	0.020	0.027	0.012	0.012	0.010	0.007	–
Fe	0.243	0.281	0.421	0.446	0.102	0.099	0.108	0.119	0.180	0.189	0.205	0.206	0.212	0.168	0.477
Mn	0.002	0.004	0.004	0.006	–	0.002	0.003	0.004	0.005	0.003	0.002	0.007	0.005	0.005	0.014
Mg	1.75	1.71	1.55	1.54	0.918	0.866	0.880	0.900	0.900	0.919	0.877	0.921	0.893	0.881	1.51
Ca	0.002	0.002	0.001	0.001	0.917	0.958	0.917	0.969	0.865	0.815	0.902	0.827	0.835	0.943	0.006
Na	–	–	–	–	0.024	0.037	0.031	0.028	0.025	0.029	0.029	0.022	0.022	0.028	–
K	–	–	–	–	–	–	0.001	–	–	–	0.001	–	–	–	0.001
Total	3.00	2.99	2.99	3.00	4.03	4.06	4.04	4.07	4.04	4.04	4.05	4.05	4.04	4.06	4.01
Mg/Mg+Fe	0.879	0.859	0.787	0.776	0.900	0.897	0.891	0.883	0.833	0.829	0.811	0.817	0.808	0.840	0.760
Ca					47.3	49.8	48.1	48.7	44.5	42.4	45.5	42.3	43.0	47.3	0.3
Mg					47.4	45.0	46.2	45.3	46.3	47.8	44.2	47.1	46.0	44.2	75.8
Fe					5.3	5.2	5.7	6.0	9.3	9.8	10.3	10.5	10.9	8.4	23.9
Rock type	T	T	P	G	T	T	T	T	P	P	P	G	G	G	P

** Total Fe as FeO Analyst, J.M. *M. Komatsu

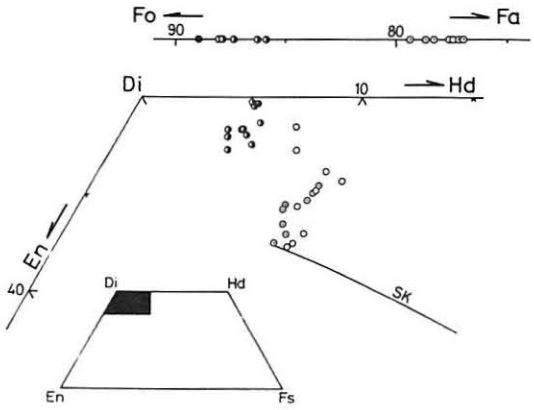

Fig. 7 Plot of Ca-rich clinopyroxene in Di-Hd-Fs-En quadrilateral. Two pyroxenes plotted between plots groups are of fine-grained gabbro. Line SK indicates pyroxene trend of Skaergaad intrusion. Symbols show host rock type.

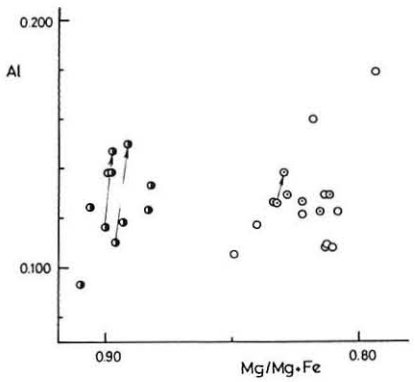

Fig. 8 Plot of clinopyroxene in Al vs. Mg/Mg+Fe diagram. Arrow indicates a compositional variation from the core to the margin.

pegmatoid intercumulus crystal accompanying a decrease of Mg ratio. The same relation exists in the cumulus pyroxene of olivine gabbro.

Cr and Ti are much more complicated. The general characteristic is an increase from the core to the margin within a single crystal in troctolite. This variation is also shown in

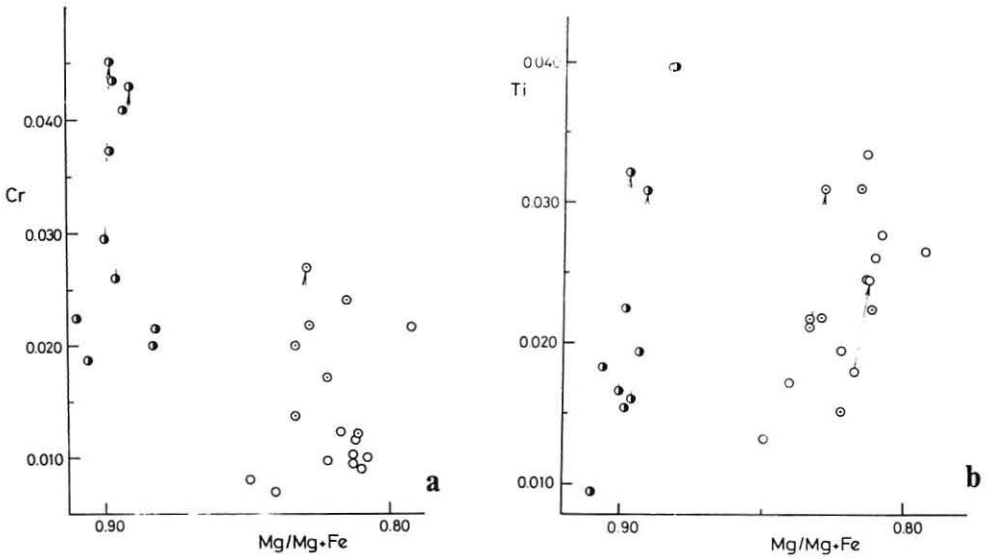

Fig. 9 a) Plot of clinopyroxene in Cr vs. Mg/Mg+Fe diagram. Arrow is the same as is in Fig. 8.
b) Plot of clinopyroxene in Ti vs. Mg/Mg+Fe diagram.

pyroxenes of the other rock group. Based on the crystal field theory proposed by Burns (1970), Campbell and Borley (1974) discussed a behavior of Cr^{3+}, Ti^{4+} and Al^{3+} in pyroxenes of the Jimberlana intrusion and concluded that Cr^{3+} and Al^{3+} are enriched in early stage pyroxenes whereas Ti^{4+} is much in the pyroxenes of a middle stage. In our clinopyroxenes, although a degree of variation is small, Cr Ti and Al tend to be rich to the margin of pyroxene. And there is a notable decrease in Cr from the troctolite pyroxene to the olivine gabbro pyroxene.

Substitution relations in the clinopyroxenes are examined in the plots in (Al + Cr – 2Ti) – (Na + K) diagram which indicates that all plots were clustered parallel to the ordinate and therefore, jadeite-kosmochlor substitution is negligible (Fig. 10a).

$(Al^{VI} + Cr) - (Al^{IV} - 2Ti)$ diagram (Fig. 10b) indicates the degree of essential tschermakitic substitution in clinopyroxene. Many scattered plots nearer to the abcissa are explained by the ferritschermackitic substitution which was indicated by the decrease of Mg ratio.

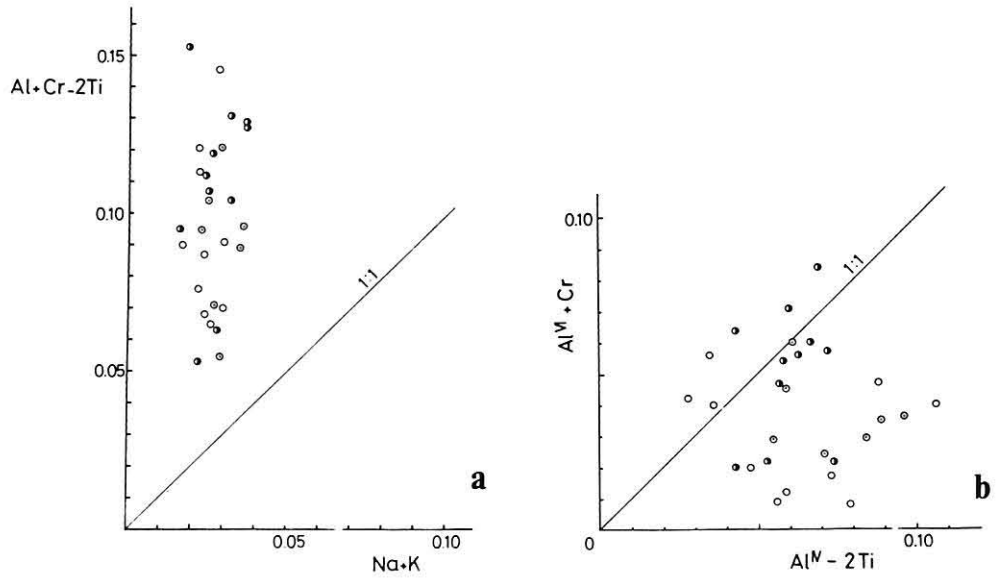

Fig. 10 a) Plot of Al+Cr–2Ti of clinopyroxene against Na+K.
b) Plot of clinopyroxene in Al^{VI}+Cr vs. Al^{IV}–2Ti diagram.

Clinopyroxene from pyroxene gabbro has an abnormal composition which is plotted between two groups (Fig. 7). The host rock itself is fine to medium-grained and it is difficult to decide whether it belongs to the cumulate or not.

The composition of orthopyroxene is poor in Ca, Al, Ti and Cr (Tab. 1., No. 11).

Amphibole: Amphibole commonly occurs at the margin of clinopyroxene as the last crystallized intercumulus mineral in the gabbros (Fig. 4). It is deep brownish in color. An EPMA analysis was carried out for the brown hornblende from troctolite (Tab. 2).

Table 2 Chemical composition of brown-hornblende from the Ameyama Gabbro.

	Amphibole	
	1	2
	Ame 13	Ame 13
SiO_2	41.9	41.9
TiO_2	4.57	4.85
Al_2O_3	12.1	11.8
Cr_2O_3	2.28	2.31
FeO*	5.34	5.62
MnO	0.02	0.04
MgO	15.8	15.7
CaO	12.3	12.4
Na_2O	2.81	2.82
K_2O	0.36	0.45
Total	97.5	97.9

Number of cation per 23 oxygens

Si	6.20	6.20
Al	2.10	2.05
Ti	0.508	0.539
Cr	0.269	0.272
Fe	0.661	0.695
Mn	0.003	0.006
Mg	3.48	3.46
Ca	1.96	1.97
Na	0.805	0.807
K	0.068	0.085
Total	16.05	16.08
Mg/Mg+Fe	0.840	0.833
Rock type	T	T

* Total Fe as FeO Analyst, J.M.

The result of analysis shows that the brown hornblende is very rich in TiO_2 (about 5 percent, Max.) and Cr_2O_3 (more than 2 percent). Therefore, this hornblende is to be defined as a chromian-kaersutite. Because of the result that Fe was all assumed to be FeO, total cation number in the analysis exceeds 16 on the basis of 0 = 23 (Robinson et al., 1971; Staut, 1972; Misch and Rice, 1975). For instance, let all Fe be FeO, total cation number is 16.052: Si = 6.199, Al^{IV} = 1.801, Al^{VI} = .302, Ti = .509, Cr = .269, Fe^{3+} - none, Fe^{2+} = .661, Mn = .003, Mg = 3.480, Ca = 1.955, Na = .805, K = .068. But if all Fe is assumed to be Fe_2O_3, total cation number decreases to 15.489: Si = 5.983, Al^{IV} = 2.017, Al^{VI} = .013, Ti = .491, Cu = .257, Fe^{3+} = .637, Fe^{2+} = none, Mn = .003, Mg = 3.359, Ca = 1.886, Na = .778, K = .165.

Dawson and Smith (1975) reported the amphibole containing 2 percent of Cr_2O_3 which differs from our amphibole in respect of negligible TiO_2 content. It is generally admitted that Cr_2O_3 content is rich in kaerusutite and titaniferous pargasite, but does not exceed 1 percent at most. The problems mentioned will be presented elsewhere.

Chemistry

The bulk chemical composition of the Ameyama rocks was determined by gravimetry for SiO_2, by chelatemetry for Al_2O_3, Fe_2O_3, CaO and MgO, spectrophotometry for TiO_2 and atomic absorption for MnO, flamephotometry for Na_2O and K_2O, FeO was determined by conventional wet method. For some of the samples, X-ray fluorescence method was applied to determine SiO_2, TiO_2, Al_2O_3, total Fe, CaO and K_2O. The result of analyses is shown in Table 3. H_2O content is very high in wehrlitic gabbro and troctolite having large amount of olivine which was variably serpentinized. The results were recalculated as water-free.

Fig. 11 indicates the variation of the main oxides on anhydrous basis against 100

Table 3 Chemical composition of the Ameyama gabbros and diabase.

	Wehrlitic Gabbro			Troctolite					Pegmatoid	Olivine Gabbro		Gabbro	Diabase		
	1	2	3	4	5	6	7	8	9	10	11	12	13	14	15
	Pip-Ame 11	Ame 2	Ame 5	Ame 13	Pip-Ame 13	Ame 12	Pip-Ame 14	Ame 14	Ame 3	A-5	A-7	A-1	Ame 15	Ame 16	A-18
SiO_2	38.03	38.49	40.04	39.24	38.34	39.50	44.92	44.84	42.25	47.42	48.06	50.95	49.89	47.57	49.35
TiO_2	0.28	0.11	0.15	0.12	0.35	0.12	0.35	0.27	0.30	0.39	0.27	0.30	1.16	1.09	2.00
Al_2O_3	4.22	5.23	6.62	14.77	13.52	12.43	22.07	21.59	9.46	13.69	18.22	16.01	16.28	16.88	15.00
Fe_2O_3	5.28	2.61	2.36	4.33	2.41	1.59	1.20	0.96	3.69	1.47	1.38	0.96	3.88	1.96	2.84
FeO	3.51	5.69	5.42	4.01	3.97	5.12	2.74	2.96	8.18	5.74	4.80	2.79	7.00	6.77	6.93
MnO	0.08	0.13	0.13	0.05	0.09	0.05	0.14	0.04	0.13	0.14	0.12	0.09	0.11	0.12	0.21
MgO	33.70	34.89	31.08	20.48	23.56	25.59	12.05	11.30	23.72	15.90	12.21	11.82	6.20	8.80	8.79
CaO	5.72	2.64	4.13	9.59	7.61	6.11	11.38	12.00	5.75	10.24	10.20	13.14	9.54	10.73	9.19
Na_2O	0.14	0.37	0.77	0.82	1.17	1.67	2.35	2.05	1.99	2.85	3.00	2.74	4.74	3.43	3.81
K_2O	0.06	0.01	0.00	0.07	0.03	0.09	0.09	0.18	0.03	0.05	0.08	0.02	0.08	0.08	0.10
P_2O_5	0.07	0.05	0.05	0.08	0.05	0.07	0.04	0.06	0.07	0.10	0.06	0.06	0.34	0.27	0.29
$H_2O(+)$	8.46	8.58	8.05	5.83	8.42	6.76	2.89	3.06	5.07	2.30	1.35	1.20	0.82	1.64	1.60
$H_2O(-)$	0.61			0.59	0.83	0.41	0.46	0.27					0.17	0.17	
Total	100.16	98.83	98.80	99.80	100.35	99.51	100.68	99.58	100.64	100.29	99.75	100.08	100.18	99.51	100.11
Analyst	S.H.	S.M.	S.M.	S.H.	S.H.	S.H.	S.H.	S.H.	S.M.	S.M.	S.M.	S.M.	S.H.	S.H.	S.M.
Norm															
	Or	0.35	0.06	–	0.42	0.18	0.53	0.53	1.06	0.18	0.30	0.47	0.12	0.48	0.48	0.59
Pl	ab	1.18	3.30	6.51	4.40	3.87	8.71	14.55	16.34	15.37	9.54	24.01	23.17	37.23	21.83	32.22
	an	10.72	12.49	14.61	36.40	31.55	24.91	49.41	49.20	16.79	24.42	36.02	31.33	22.89	30.40	23.54
	WO	7.19	0.12	2.32	4.43	2.45	–	2.83	2.67	4.70	10.74	5.92	13.97	9.28	8.78	8.41
Di	en	6.12	0.09	1.86	3.54	1.99	–	2.23	2.07	3.53	7.92	4.31	10.94	5.78	5.75	5.77
	fs	0.15	–	0.19	0.37	0.17	–	0.28	0.31	0.70	1.79	1.06	1.49	2.94	2.42	1.97
Hy	en	0.85	8.77	7.72	–	–	–	–	–	–	–	–	2.63	–	–	5.00
	fs	–	0.84	0.80	–	–	–	–	–	–	–	–	0.39	–	–	1.70
Ol	fo	53.90	54.67	47.52	33.46	39.71	44.66	19.46	18.27	38.91	22.19	23.22	11.12	6.74	11.33	7.79
	fa	1.22	5.79	5.41	2.55	3.65	6.15	2.66	3.06	8.51	5.52	4.94	1.66	3.86	5.26	2.93
	C	–	–	–	–	–	0.45	–	–	–	–	–	–	–	–	–
	Ne	–	–	–	1.37	3.27	2.75	2.88	0.56	0.79	2.47	0.74	–	1.54	3.90	–
	mt	7.66	3.78	3.42	6.28	3.49	2.31	1.74	1.39	5.35	2.13	2.00	1.39	5.63	2.84	4.12
	il	0.53	0.21	0.28	0.23	0.66	0.23	0.66	0.51	0.57	0.74	0.51	0.57	2.20	2.07	3.80
	ap	0.16	0.12	0.12	0.19	0.12	0.16	0.09	1.39	0.16	0.23	0.14	0.14	0.79	0.63	0.67

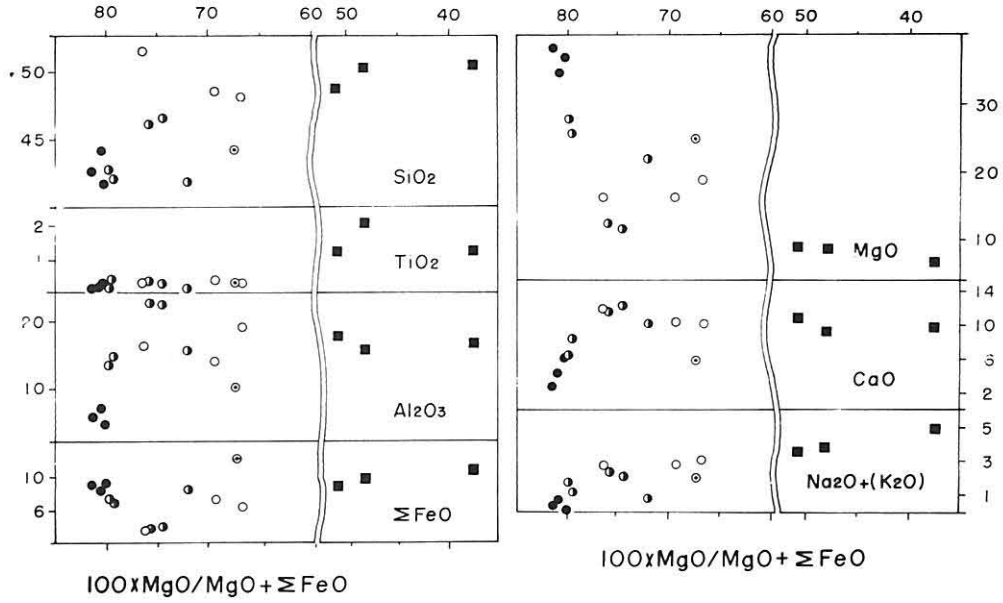

Fig. 11 Variation of the main oxides against 100X MgO/MgO + ΣFeO ratio.

MgO/(MgO + Total Fe as FeO) ratio results in a marked scattering due to a wide range of the ratio within each rock group. As the ratio decreases, SiO_2 shows an increase from wehrlitic gabbro to troctolite and to olivine gabbro. Al_2O_3 shows a rapid increase from wehrlitic gabbro to troctolite and then decreases in olivine gabbro. The same tendency is seen with CaO. The variation of Na_2O (+ K_2O) is an increase. A notable decrease is displayed by the variation of MgO and ΣFeO in wehrlitic gabbro-troctolite.

On the other hand, the plots of diabase show smooth trend in which SiO_2, ΣFeO and Na_2O increase with a decrease of the ratio and Al_2O_3 and MgO slightly decrease with the ratio.

The rock compositions are plotted on an A-F-M diagram and are compared with those of the cumulus rocks of the Western Zone of the Hidaka Metamorphic Belt and with the Western Marginal Zone diabases which are free from spilitization (Fig. 12a).

For the cumulus rocks, the Ameyama rocks are plotted nearer the apex M than the cumulates of the Western Zone of the metamorphic belt; the Mt. Poroshiri rocks. The plots of wehrlitic gabbro and troctolite are roughly aligned on areas parallel to the A-M side and in the direction shown in the layered rocks of wehrlite to anorthosite in Mt. Poroshiri (Unpublished data). Olivine gabbro may be situated on similar trend but might show somewhat different trend if sufficient analyses were available. Some Fe enrichment exists in each rock group, the Ameyama gabbros were probably formed by a fractional accumulation of olivine and of plagioclase without a marked compositional change which is shown in term of MgO-CaO-Al_2O_3 diagram (Fig. 12b). The proportion of the accumulated olivine and plagioclase, separates troctolite into two. The appearance of new additional phase,

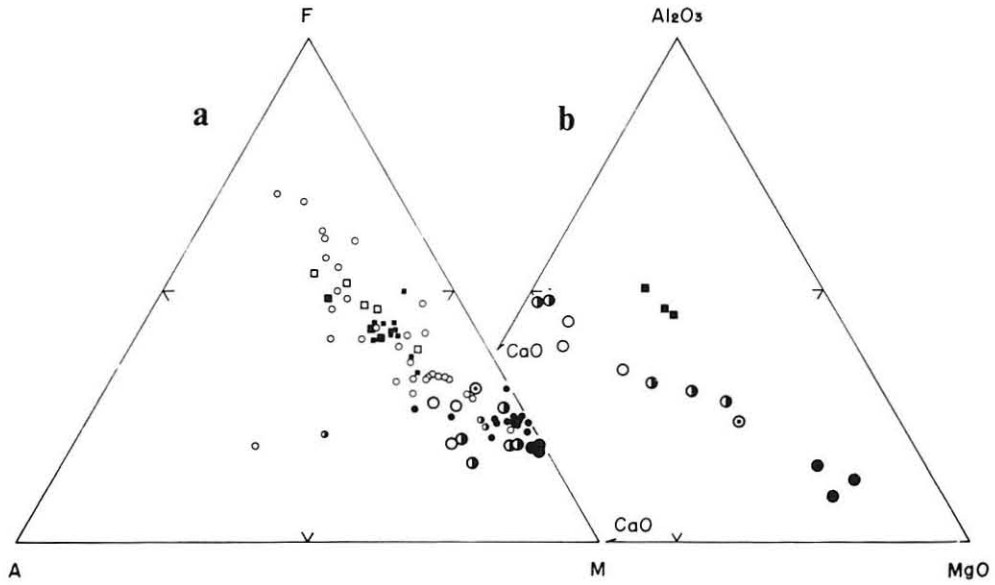

Fig. 12
a) A-F-M plot of the Ameyama gabbros and diabase.
Large circle and square indicate the Ameyama rocks. Small ones are of Mt. Poroshiri rocks (Hashimoto, 1975., Miyashita, unpublished data) and of the Western Marginal Zone diabase (Suzuki, 1977).
b) Plots of the Ameyama rocks on $CaO - Al_2O_3 - MgO$ diagram.

clinopyroxene, push back olivine gabbro in between.

The plots of the Ameyama diabase shown in Fig. 12a make a smooth trend which appears to be more sodic than the diabases of the Western Marginal Zone of the Hidaka Belt.

In SiO_2-Alkalies diagram (Fig. 13) which suggests the magma type from which the rocks were crystallized, the Ameyama diabase is on the line proposed to divide a tholeiitic from an alkali-basalt by MacDonald and Katsura (1964). The main groups of diabase in the Axial Zone of Hokkaido were also plotted for comparison. The diabases of the Western Marginal Zone of the Hidaka Belt are plotted on the both fields. Swarm of the Shimokawa diabases cropping out in the Northern Hidaka Belt, cluster in the tholeiitic field. On the other hand, the Kamuikotan diabases which are accompanied by greenschists and blueschists, are plotted exclusively in the alkali-basalt field.

In SiO_2-Alkalies diagram, the plots of the cumulates scattered roughly along the line, do not represent the magma composition, but there is a good agreement in their proportion of Na_2O content ($Na_2O/Na_2O + K_2O$) between the cumulate and the diabase: wehrlitic gabbro 0.89 in average, Troctolite 0.94, Olivine gabbro and gabbro 0.98 Pegmatoid 0.99, and Diabase 0.98.

The correspondence in high soda content in the Ameyama rocks favours to suggest their original magma stem from which the cumulate and the diabase were derived.

The minor contents of Ni and Cr were determined by atomic absorption method. The result was plotted in Ni versus Cr diagram and was compared with Ni-Cr of the basic plutonic

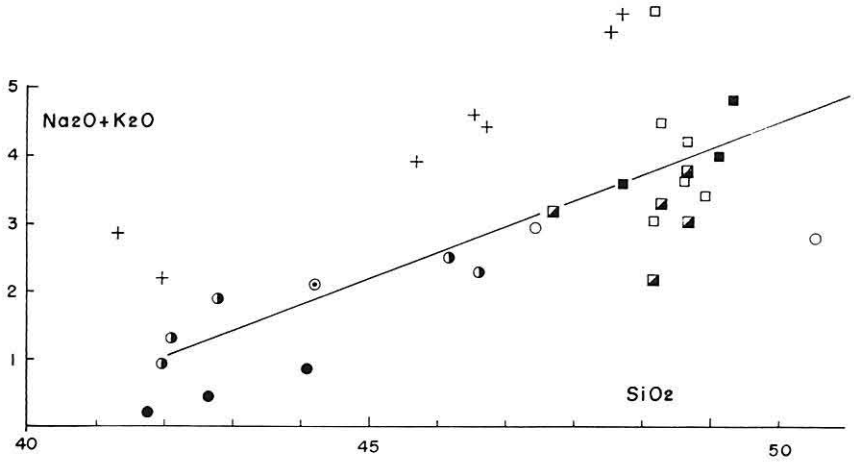

Fig. 13 Plot of $Na_2O + K_2O$ against SiO_2.
The line indicates a boundary of alkaline-basalt and tholeiitic basalt by MacDonald and Katsura (1964). Filled circle: Wehrlitic grbbro. Half-filled circle: Troctolite. Circle with dot: Pegmatoid. Open circle: Olivine gabbro and Gabbro. Filled square: The Ameyama diabase. Open square: Diabase of the Western Marginal Zone of the Hidaka Belt (Suzuki, 1977). Half-filled square: The Shimokawa diabase. Cross: The Kamuikotan diabase (Bamba and Sawa, 1967., Bamba, 1974).

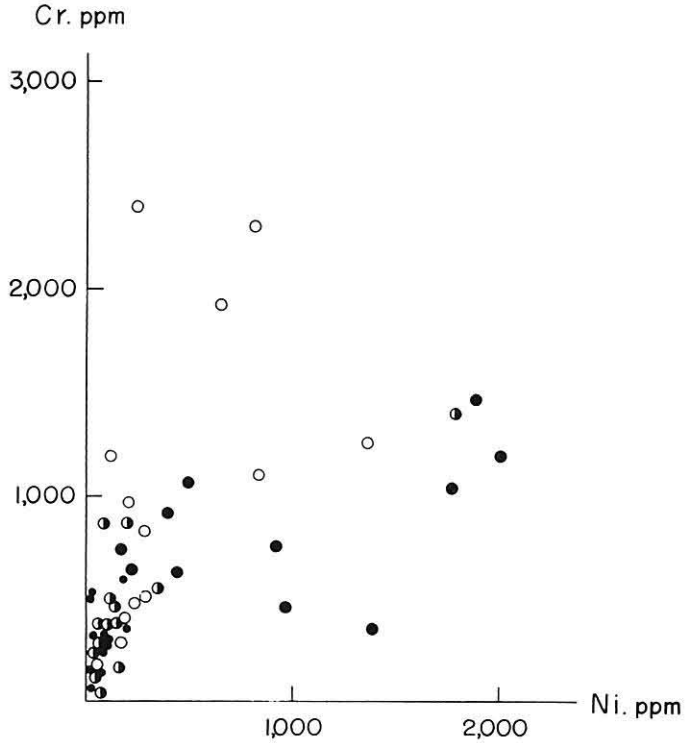

Fig. 14 Cr vs. Ni variation diabram of basic plutonic rocks of the Hidaka Metamorphic Belt.
Filled circles: The Ameyama rocks. Open circles: Mt. Poroshiri rocks of the Western Zone. Half filled circles: Synkinematic intrusives of the Axial Zone. Dots: Late-kinematic intrusives of the Eastern Zone. (Analyst, S.H. and S.M.)

rocks of the Hidaka Metamorphic Belt (Fig. 14). Plots indicate that the Ameyama gabbros show a tendency to Ni enrichment, while the Mt. Poroshiri rocks tend to be rich in Cr content. The other rocks show a cluster within 1000 ppm Cr and 400 ppm Ni content.

Conclusion

(1) The cumulates cropping out in the Hidaka Metamorphic Belt are characterized by the occurrence of tectonic sheets or blocks and are formed prior to the main phases of plutonic intrution. Thè Ameyama gabbros have close similarities to the layered rocks of the Western Zone of the Metamorphic Belt in mineralogy and chemical characteristics. A dominant accumulation of olivine and/or An rich plagioclase is followed by the formation of clinopyroxene, cumulus or intercumulus or both. Cr-spinel is the earliest phase of crystallization.

(2) The diabase accompanied by the gabbros differs from the Kamuikotan diabase and the Shimokawa diabase in chemical characteristics. That the Ameyama diabase is highly sodic, might indicate a linkage to the Ameyama gabbros which is also sodic in nature.

(3) Clinopyroxenes of the Ameyama gabbros are rich in Cr and Ti. Substitution relation is dominant in tschermackitic type. Noteworthy is the fact that Cr, Ti and Al are enriched at the margin of the crystal.

(4) The brown hornblende in the gabbro is chromian kaersutite. It has been generally accepted that kaersutite occurs characteristically in an alkaline rock. As the Ameyama gabbros seemed not to be derived from an alkaline basic magma, a peculiar composition of the amphibole might have been controlled by specific P-T condition of crystallization (Helz, 1973) or by local concentration of alkaline residual liquid.

Acknowledgements

We wish to thank to Professor M. Minato for his continuing encouragement and advice. Special thanks are due to Prof. M. Shimazu and Dr. M. Komatsu of the Niigata University, for their valuable help during EPMA analyses. We would like to thank to Dr. S. Yamazaki of the Agricultural Experimental Station, Hokkaido, for his assistance in the X-ray fluorescence analyses. Mr. H. Ohta and Miss C. Sato helped us in preparing diagrams and manuscripts.

References

Bamba, T. 1974. A series of magmatism related to the formation of the spilites. In: Amstrutz, G.C. (Ed.), *Spilites and Spilitic Rocks.* pp.83-112, Spiringer-Verlag. Berlin. Heidelberg. New York.

Bamba, T. and Sawa, T., 1967. Spilite and associated manganiferous hematite deposits of the Tokoro district, Hokkaido, Japan. *Rept.* No. 221, Geol. Surv. Japan.

Burns, R.G., 1970. *Mineralogical Applications of Crystal Field Theory.* Cambridge Univ. Press.

Campbell, I.H. and Borley, G.D., 1974. The geochemistry of pyroxenes from the lower layered series of the Jimberlana Intrusion, Western Australia. *Contr. Mineral. Petrol.*, 47: 281-297.

Dawson, J.B. ans Smith, J.V., 1975. Chromite-silicate intergrowth in upper-mantle peridotites. *Phys. Chem. Earth,* 9: 339-350.

Hashimoto, S., 1975. The basic plutonic rocks of the Hidaka Metamorphic belt. *Jour. Fac. Sci. Hokkaido Univ.*, ser. IV, 16: 367-420.

Hashimoto, S., 1976. Structural significance of the Western Zone of the Hidaka Metamorphic Belt. *Rept. Geol. Min. Niigata Univ.*, 4: 409-414. (Japanese with English abstract)

Helz, R.T., 1973. Phase relation of basalts in their melting range at PH_2O = 5 kb as a function of oxygen

fugacity: Part I. Mafic phases. *Jour. Petrol.*, 14: 249-302.
MacDonald, G.A. and Katsura, T., 1964. Chemical composition of Hawaiian lava. *Jour. Petrol.*, 5: 82-133.
Misch, P. and Rice, J.M., 1975. Miscibility of tremolite and hornblende in progressive Skagit Metamorphic Suite, North Cascades, Washington. *Jour. Petrol.*, 16, 1-21.
Miyashita, S. and Hashimoto, S., 1975. The layered basic complex of Mt. Poroshiri, Hokkaido, Japan. *Jour. Fac. Sci. Hokkaido Univ.*, ser. IV, 16, 421-452.
Robinson, P., Ross, M. and Jaffe, H.W., 1971. Composition of the anthophyllite-gedrite series, comparisons of gedrite and hornblende, and the anthophyllite-gedrite solvus. *Amer. Min.*, 56, 1005-1041.
Sinno, I. and Hayashi, M., 1976. Chemical composition and d_{130}-spacing of olivine. *Jour. Miner. Soc. Japan*, 12, 194-205.
Stout, J.H., 1972. Phase petrology and mineral chemistry of coexisting amphiboles from Telemark, Norway. *Jour. Petrol.*, 13, 99-145.
Suzuki, M., 1977. Characteristics of diabase and spilitic rocks in the axial region of Hokkaido and genesis of spilite. *Rep. Geol. Surv. Hokkaido*, 49, 1-36. (in Japanese with English abstract)
Wager, L.R., Brown, G.M. and Wadsworth, W.J., 1960. Types of igneous cumulates. *Jour. Petrol.*, 1, 73-85.

(Received on Oct. 31, 1978)